

[OII] λ 3727 Emission from the Companion to the Quasar BR 1202-0725
at $z=4.7$

Kouji OHTA, Tsuyoshi MATSUMOTO, and Toshinori MAIHARA

Department of Astronomy, Kyoto University, Sakyo-ku, Kyoto 606-8502

E-mail(KO): ohta@kusastro.kyoto-u.ac.jp

Fumihide IWAMURO, Hiroshi TERADA, Miwa GOTO, Kentaro MOTOHARA,

Tomoyuki TAGUCHI, and Ryuji HATA

Department of Physics, Kyoto University, Sakyo-ku, Kyoto 606-8502

Michitoshi YOSHIDA

Okayama Astrophysical Observatory, National Astronomical Observatory,

Kamogata-cho, Okayama 719-0232

Masanori IYE

National Astronomical Observatory, Mitaka, Tokyo 181-8588

and

Chris SIMPSON, Tadafumi TAKATA

Subaru Telescope, National Astronomical Observatory of Japan,

Hilo, Hawaii 96720, USA

(Received 1999 December 8; accepted 2000)

Abstract

Results of a narrow-band imaging for the redshifted [OII] λ 3727 emission around a quasar at $z = 4.7$ obtained with the Subaru telescope and CISCO (a Cassegrain near infrared camera) are presented. A significant emission line is detected in the narrow-band H₂ ($v = 1 - 0$ S(1)) filter at a location $\sim 2.''4$ northwest from the quasar, where the presence of a companion has been reported in Lyman α emission and the rest-frame UV continuum. We identify this line as [OII] λ 3727 emission and confirm that the source

really is a companion at $z = 4.7$. The [OII] $\lambda 3727$ flux from the companion is estimated to be 2.5×10^{-17} erg $s^{-1} \text{ cm}^{-2}$. If the companion is a star forming object, the inferred star formation rate is as high as 45-230 $M_{\odot} \text{ yr}^{-1}$ even without assuming the extinction correction. This value is higher than those derived from the Lyman α emission or from the UV continuum. Thus, provided that the difference is caused by dust extinction, the extinction corrected star formation rate is calculated to be 45 to 2300 $M_{\odot} \text{ yr}^{-1}$ depending on the assuming extinction curves.

Key words: Galaxies: formation — Quasars: formation — Quasars: individual (BR 1202–0725)

1. Introduction

There are growing numbers of observational and theoretical suggestions that high redshift quasars are under intense star burst and are related to an early phase of galaxy formation (e.g., Djorgovski et al. 1999; Haehnelt, Rees 1993). BR 1202–0725 at $z=4.7$ is one of the most distant quasars known to date and provides us a unique opportunity for studying galaxy formation process and its relationship to the quasar activity. The quasar has an optical (rest UV continuum) companion located at $\sim 2.''4$ northwest from the quasar and it is also seen in Lyman α emission (Djorgovski 1995; Hu et al. 1996; Petitjean et al. 1996; Fontana et al. 1996). The projected distance between the companion and the quasar is ~ 14 kpc. (We use a cosmological parameter set of $q_0 = 0.5$ and $H_0 = 50$ $\text{km s}^{-1} \text{ Mpc}^{-1}$ throughout this paper.) The flux of the Lyman α emission is estimated to be $(1.5 \sim 2.5) \times 10^{-16}$ $\text{erg s}^{-1} \text{ cm}^{-2}$ (Hu et al. 1996; Petitjean et al. 1996). If the Lyman α emission is attributed to star formation, an expected star formation rate is 28-47 $M_{\odot} \text{ yr}^{-1}$. A high angular resolution image in I_{814} -band taken with the Hubble Space Telescope (HST) shows that the companion has an elongated structure toward the quasar; it may be tidally interacting with the quasar and may be merging into the host galaxy (Hu et al. 1996).

Another important aspect in this system is the presence of a huge amount of molecular gas and dust. CO emission lines from this system is detected by Ohta et al. (1996) and Omont et al. (1996b) and the dust thermal emission by McMahon et al. (1994), Isaak et al. (1994), Omont et al. (1996a), and more recently by Benford et al. (1999). The estimated mass of the molecular gas amounts up to $\sim 10^{11} M_{\odot}$, which is comparable to a stellar mass of a present-day giant elliptical galaxy. Presence of such an amount of molecular gas implies that the system is considered to be under intense star burst ($\sim 10^3 M_{\odot} \text{ yr}^{-1}$), i.e., under a forming phase in the early universe. Distributions of the

dust and the molecular gas show a double peak structure; 1.35 mm continuum and CO emission show a peak at the quasar position and at $\sim 4''$ northwest of the quasar (Omont et al. 1996b; Kawabe et al. 2000). The intensity of the emission is roughly comparable with each other. There is no optical counterpart at the northwestern position; the optical companion is located between the quasar and the dust/molecular companion. A recent high angular resolution radio continuum map obtained with the Very Large Array also shows the double peak structure at 1.4 GHz (Yun et al. 2000), and the star formation rate is estimated to be again $\sim 10^3 M_{\odot} \text{ yr}^{-1}$, by assuming that the radio continuum emission traces star formation activity which is inferred from the fact that the spectral energy distribution longward of far-infrared is quite similar to that of the central region of M 82 (Kawabe et al. 1999; Yun et al. 2000).

The Lyman α emission from the companion of the quasar is probably quenched very much not only due to dust extinction at UV wavelength but also due to the resonance scattering, thus emission lines at longer wavelength are more suitable to trace star formation activity. Further, a number of high redshift Lyman α emitters have been found (e.g., Pascarelle et al. 1996; Hu & McMahon 1996; Cowie & Hu 1998, Thommes et al. 1998), but the degree of extinction in these systems is hardly examined. Thus the determination of fluxes of other emission lines in this system would provide us an insight for the amount of dust obscuration and a more reliable star formation rate for these Lyman α emitters.

The [OII] λ 3727 emission from the companion of BR1202-0725 is redshifted to $2.123\mu\text{m}$, which lies very close to the rest wavelength of H_2 ($v = 1 - 0 \text{ S}(1)$) emission. We used hence a narrow-band filter for this line to produce a monochromatic [OII] λ 3727 image of the BR1202-0725, using the Subaru telescope and CISCO (near infrared imaging spectrograph at the Cassegrain focus). Here we report the detection of [OII] λ 3727 emission line from the companion and possible other companions.

2. Observations and Data Reduction

Observations were made with CISCO (Motohara et al. 1998) attached to the Cassegrain focus of the Subaru telescope on 1999 March 4, April 1, and April 2, during a period of test observing run for the instrument and the telescope. Since the weather condition was not good on March 4, we used only the data taken in April. Detector used was a 1k by 1k HgCdTe array with the pixel scale of $0.''116$, giving a field of view of $\sim 2'$. Narrow-band [OII] line imaging with a filter centered at $2.1196\mu\text{m}$ with a FWHM of $0.0199\mu\text{m}$ (the transmission between $2.113\mu\text{m}$ and

2.126 μm ranges from 80% to 88%) at 77 K and K' (1.96 – 2.30 μm) imaging were carried out. The images were taken with an octagonal dither pattern of which diameter is $\sim 20''$, and six frames were taken at each telescope pointing. The offsets were introduced to reduce non-uniformity of the pixel sensitivity. The exposure time for each frame was 50 sec for the narrow-band imaging and 10 sec or 20 sec for the K' imaging. The total exposure times were 1200 sec on Apr. 1 and 2400 sec on Apr. 2 for the narrow-band imaging, and 480 sec both on Apr. 1 and Apr. 2 for the K' imaging. Seeings during the observations were $\sim 0.''6$ to $\sim 1.''0$ (FWHM) and $\sim 0.''3$ to $\sim 0.''6$ (FWHM) on Apr. 1 and Apr. 2, respectively.

Data reduction was made with IRAF¹. For each frame, the frame taken at the next pointing of the telescope was subtracted; since six images were taken at one pointing position, for the n-th frame in a pointing, the n-th frame in the next pointing was subtracted. For the last pointing data, we subtracted the frames taken before that pointing. The small scale dark pattern was eliminated by this procedure. The residual of the background shows a smooth distribution in each quadrant of the detector. Thus we fitted a two dimensional polynomial function of fourth order in x -direction and third in y -direction with cross terms to the residual background in each quadrant, and subtracted it. The background of the images became flat and zero at this stage, except for the first 6 frames in each night presumably due to some unstable condition of the readout of the detector at that time. The standard K' sky frame made from many observing runs was applied for flat fielding at this stage both for the K' data and the narrow-band data, because the narrow-band was actually inside in a part of the K' -band. To check the robustness of the result, we also examined the case without applying the flat fielding for the narrow-band data. The discrepancy between the two procedures is not significant, but a flux of the companion discussed below is 8 % smaller for the latter case. It should be noted that the flat fielding error does not affect the present results and discussion described below so much, because we used the quasar as a calibrator and the global variation in the flat frame must be insignificant between the quasar position and the companion position. In addition, the pixel to pixel variation is reduced much for the photometry since a relatively large (8 pixel diameter) aperture was used in this study.

The images were then shifted and smoothed with a Gaussian kernel to match the seeing size. We discarded poorer frames with a seeing size (FWHM) larger than 8.57 pixel (0.''99) for the data taken on Apr. 1 and 4.98 pixel (0.''58) for the data taken on Apr. 2. Finally the images were stacked to make the final image, excluding the first 6 frames,

¹ IRAF is distributed by the National Optical Astronomy Observatories, which is operated by the Association of Universities for Research in Astronomy, Inc. under cooperative agreement with the National Science Foundation.

and the resulting narrow-band image obtained on Apr. 2 is shown in figure 1. (In figure 1, a slight smoothing was applied for clearer presentation.) The total effective integration times for the narrow-band imaging are 900 sec for Apr. 1 data and 1900 sec for Apr. 2 data. The corresponding effective integration time for the broad band filter was 420 sec both for Apr. 1 and Apr. 2 data.

In figure 1, the companion is seen at $\sim 2.''4$ northwest of the quasar. In order to examine the reality of the presence of the companion in the narrow-band image, we divided the data (Apr. 2 data) into the first half and the last half. Although the resulting combined images have lower signal-to-noise ratios, the feature is still seen in both images. For a further test, combined images were constructed by discarding the frames which were obtained at a telescope pointing in order to avoid influence by some spurious feature at a particular position in the detector (e.g., hot pixel). For the Apr. 2 data, since we used seven pointing data for figure 1, we combined six pointing data into one image. The resulting seven images are displayed in figure 2 without smoothing. In every image, the companion is detected significantly, thus a spurious feature at a particular position in the detector does not produce the companion feature. The FWHM of the companion feature measured by Gaussian fitting is 10 to 20 % larger or smaller than that of the quasar in each image of figure 2. The difference is considered to be attributed to the low signal-to-noise ratio.

Another possible cause for a fake companion is a ghost of the quasar. If the companion feature was the ghost, its position relative to the quasar depends on the position of the object in the detector, i.e., the telescope pointing. We combined the frames taken in the western and eastern regions of the detector with respect to its center, respectively. Twenty one frames taken in the eastern region in the detector were combined in one image and is shown in the left panel of figure 3. Similarly, seventeen frames taken in the western region was combined into one image and is shown in the right panel of figure 3. In both images, the companion feature is located at $2.''4 \pm 0.''1$ northwest of the quasar. Thus we conclude the companion feature is not the ghost image.

We also reduced the data independently using another manner of the data reduction which is adopted by Iwamuro et al. (2000) for near-infrared observations of the Hubble Deep Field North with the CISCO. Although the morphology of the feature is slightly different, the existence of the companion in the image is as clear as that in figure 1. A count rate for the companion is different from that obtained above by about 10%. Therefore we conclude that the companion feature is real.

The flux calibration for the narrow-band imaging was made using the filter transmission curve under the cooled condition and a K -band spectrum of the quasar BR 1202-0725 taken with the CGS-4 in the UKIRT service observing

run in 1996. The slit width used was $1.''23$ and total exposure time was 32 min. Flux calibration was made using UKIRT standard BS4533 observed in the same observing run. The K -band spectrum shows only a continuum and the mean continuum flux level agrees well within $\sim 15\%$ with the K' magnitude obtained by Hu et al. (1996) and no significant emission lines is seen in the filter transmission. The flux calibration was done by comparing count rates of the quasar and the companion; the uncertainty of the count rate ratio estimated though figure 2 is about 10%. We suppose that the origin of the feature in the narrow-band image is $[\text{OII}]\lambda 3727$ emission as described below, and assume that the shape and the redshift of the $[\text{OII}]$ emitter are the same as those for the Lyman α emission obtained by Petitjean et al. (1996).

3. Results

3.1. The northwestern companion

As seen in the narrow-band image of figure 1, the highest peak position of the companion at the northwest of the quasar is located at $2.''4$ from the quasar, which is different from the reported position of the Lyman α emission region by $0.''2$, but the entire position of the companion is considered to agree well with those of the Lyman α companion and the optical continuum feature. (The position of the Lyman α companion coincides with that of the continuum feature (Hu et al. 1997).) The extent of the companion is $1''$ to $2''$ and the feature is concentrated within a $0.''5$ region. The elongated structure seen in the HST I -band image is not seen, though the signal-to-noise ratio is not sufficient to discuss the shape of the companion. The total counts (ADU) of the companion in figure 1 in an aperture with a diameter of 8 pixels ($0.''93$) is ~ 110 with a peak value of ~ 4 counts. A fluctuation of total counts in the same aperture evaluated in blank fields around the quasar is ~ 20 counts with a mean of about 0. Thus the significance of the feature is estimated to be about 5 sigma. The data taken on Apr 1, however, do not show the presence of this feature significantly, because of the shorter exposure time and the poorer seeing condition. In fact, the image constructed from the data taken on Apr. 2 by adjusting the exposure time to 900 sec and seeing size to $0.''99$ does not show the significant feature of the companion. (Thus we did not combine the data taken on Apr. 1.) Our K' -band image is not deep enough to detect the companion; the K -band flux density of the companion is $1.9 \times 10^{-20} \text{ erg s}^{-1} \text{ cm}^{-2} \text{ \AA}^{-1}$ (Hu et al. 1996) and is lower than our detection limit.

The flux of the companion feature in the narrow-band image (in the circular aperture of 8 pixels or $0.''93$) is

$2.5 \times 10^{-17} \text{ erg s}^{-1} \text{ cm}^{-2}$, while the contribution from the continuum is about 10 times smaller than this value as mentioned above. Therefore, considering the good positional coincidence to the Lyman α emitter and the continuum features, we identify the companion seen in the narrow-band image with the [OII] λ 3727 emitter at $z = 4.7$. The estimated observed equivalent width for the [OII] λ 3727 emission is $\sim 1300 \text{ \AA}$, that corresponds to the rest equivalent width of $\sim 230 \text{ \AA}$. The obtained [OII] λ 3727 flux is slightly lower than the upper limit set by Pahre and Djorgovski (1995) obtained with the NIRC (near infrared camera) at the Keck telescope. The non-detection with the NIRC may be due to a combination of the lower transmission of the narrow-band filter for H₂(1 – 0) line (Teplitz et al. 1998), a shorter integration time (1080 s), and a larger seeing size (typically 0.''75).

3.2. *The southwestern companion and other companion candidates*

In the *I*-band image obtained with the HST, there is another extended optical feature pointing radially to the quasar at $\sim 3''$ southwest from the quasar (Hu et al. 1996). No significant emission was detected toward this SW companion. The 3σ upper limit on this position is $\sim 1.4 \times 10^{-17} \text{ erg s}^{-1} \text{ cm}^{-2}$ with the aperture of 8 pixels (0.''93), provided that the velocity feature is the same as that of the Lyman α emission of the northwestern companion. Hu et al. (1997) reported a detection of Lyman α emission toward this companion as well as [OII] λ 3727 emission which was observed with UH 1k by 1k IR camera attached to the Canada-France-Hawaii Telescope. (They did not present the flux data.) Our result does not confirm the [OII] emission toward the SW companion. Since no significant dust thermal emission, CO emission, and radio continuum emission are detected at this position, the object might not be placed at $z = 4.7$ or be a chemically unevolved and less extinguished object with a relatively low intrinsic star formation rate.

In figure 1, there may be other [OII] λ 3727 emission regions around the quasar: at $\sim 1.''5$ south-by-east and $\sim 1.''5$ south-by-west from the quasar. Although these features are also seen in figures 2 and 3, they are very close to the quasar and might be outskirts of the point spread function. There might be another companion at $\sim 1''$ to $2''$ south from the companion. If these features are real, their close projected distances from the quasar of about 10 to 20 kpc suggest that they may be subgalactic clumps under active star formation merging into a galaxy, the host of the quasar. Alternatively, they might be gas clumps ionized by the quasar that are merging into the host galaxy. However, since all these features have the low signal-to-ratios, deeper imaging and spectroscopic observations are obviously needed to examine the existence of them and to discuss these possibilities.

4. Discussion

There are alternative interpretations for the origin of the emission line in the northwestern companion: one is a star forming object and the other one is a photoionized gas illuminated by the quasar. Petitjean et al. (1996) discussed both possibilities by constructing model continuum spectra with emission lines. In the star forming object hypothesis, they assumed a star formation rate of $13 M_{\odot} \text{ yr}^{-1}$ and 0.1 solar abundance without dust extinction. (They used $q_0 = 0.5$ and $H_0 = 75 \text{ km s}^{-1} \text{ Mpc}^{-1}$.) A shortcoming for this model arises from the fact that contribution from Lyman α emission in the model is smaller than the observed value to account for intensities of continuum and emission lines simultaneously. In the photoionization model, the model V -band flux is too small and the Lyman alpha emission is too strong (about one order of magnitude larger than the observed value). In the latter model, a strong $\text{NV}\lambda 1240$ and $\text{CIV}\lambda 1549$ emission line should be seen in the spectrum of the companion. However the spectrum of the companion by Petitjean et al. (1996) seems not to show the $\text{NV}\lambda 1240$ emission, and Hu et al. (1997) reported the absence of $\text{CIV}\lambda 1549$ emission line in the companion. Thus the identification of the northwestern companion with a star forming object seems to be more plausible.

The star formation rate estimated from the $[\text{OII}]\lambda 3727$ emission luminosity is 45 to $230 M_{\odot} \text{ yr}^{-1}$ depending on the adopted conversion factor from the $[\text{OII}]\lambda 3727$ luminosity to the $\text{H}\alpha$ luminosity (Gallagher et al. 1989; Kennicutt 1992) without extinction correction. The star formation rate estimated from Lyman α luminosity is $28\text{-}47 M_{\odot} \text{ yr}^{-1}$ under the case B recombination assumption ($L(\text{Lyman } \alpha)/L(\text{H}\alpha) = 8.7$) (Hu et al. 1996; Petitjean et al. 1996). The star formation rate estimated from the rest UV continuum (around 1400 \AA) (Madau et al. 1998) also gives a value of $22 M_{\odot} \text{ yr}^{-1}$. The star formation rate derived from the $[\text{OII}]$ emission is larger than those estimated from the Lyman α emission and the UV continuum by a factor of up to ~ 10 .

The origin of the discrepancy must be due to the severer dust extinction to the Lyman α emission and the UV continuum. By assuming that the extinction corrected star formation rate derived from the $[\text{OII}]$ luminosity is equal to that from the Lyman α luminosity, the amount of extinction in the companion can be estimated. The estimated visual extinction (A_V) ranges from ~ 0 to 1.3 mag for the Milky Way type extinction curve (Scheffler and Elsässer 1988), ~ 0 to 0.5 mag for the SMC type extinction curve (Calzetti et al. 1994), and ~ 0 to 1.1 mag for the Calzetti type extinction curve (Calzetti 1997), by assuming $A_V = 3E(B - V)$. Thus the extinction at $[\text{OII}]\lambda 3727$ emission is estimated to be ~ 0 to 2.5 mag, and the extinction corrected star formation rate amounts to 45 to $2300 M_{\odot} \text{ yr}^{-1}$.

The emission line region is adjacent to the thermal dust emission and the CO emission line region which must also be an intense star forming region at which the star formation rate inferred from the CO luminosity and the radio continuum luminosity is at the order of $1000 M_{\odot} \text{ yr}^{-1}$. The [OII] emitting region may be a less obscured region of the starburst object. However, the huge value of the estimated star formation ratio ($\sim 2000 M_{\odot} \text{ yr}^{-1}$) for the companion alone may indicate that at least a part of the [OII] emission does not come from star formation, but from the ionized gas illuminated by the quasar. Deep spectroscopic observations of the companion are required to examine a fraction of the contribution from the ionization by the quasar.

It is our great pleasure to thank Subaru telescope team for their enormous efforts for the construction of the telescope. K.O. is supported by grant-in-aid from the Ministry of Education, Science, Sports and Culture of Japan (117401230).

References

- Benford D.J., Cox P., Omont A., Phillips T.G., McMahon R.G. 1999, *ApJ* 518, L65
- Calzetti D. 1997, *AJ* 113, 162
- Calzetti D., Kinney A.L., Storchi-Bregmann T. 1994, *ApJ* 429, 582
- Cowie L.L., Hu E.M. 1998, *AJ* 115, 1319
- Djorgovski S.G. 1995, in *Science with the VLT*, eds J.R. Walsh, I.J. Danziger, (Springer Verlag, Berlin) p351
- Djorgovski S.G., Odewahn S.C., Gal R.R., Brunner R., Carvalho R.R. 1999, in *Photometric Redshifts and the Detection of High Redshift Galaxies*, eds R. Weymann, L. Storrie-Lombardi, M. Sawicki, R. Brunner, (Astronomical Society of Pacific, San Francisco) in press
- Fontana A., Cristiani S., D'Odorico S., Giallongo E., Savaglio S. 1996, *MN* 279, L27
- Gallagher J.S., Bushouse H., Hunter D.A. 1989, *AJ* 97, 700
- Haehnelt M., Rees M.J. 1993, *MN* 263, 168
- Hu E.M., McMahon R.G. 1996, *Nature* 382, 231
- Hu E.M., McMahon R.G., Egami E. 1996, *ApJ* 459, L53
- Hu E.M., McMahon R.G., Egami E. 1997, in *the Hubble Space Telescope and the High Redshift Universe*, eds N.R. Tanvir, A. Aragón-Salamanca, J.V. Wall, (World Scientific, Singapore), p91
- Isaak K.G., McMahon R.G., Hills R.E., Withington S. 1994, *MN* 269, L28
- Iwamuro F., Motohara K., Maihara T., Iwai J., Tanabe H., Taguchi T., Hata R., Terada H., et al. 2000, *PASJ* in press
- Kawabe R., Kohno K., Ohta K., Carilli C. 1999, in *Highly Redshifted Radio Lines*, eds. C.L. Carilli, S.J.E. Radford, K.M. Menten, G.I. Langston, (Astronomical Society of Pacific, San Francisco), p48
- Kawabe R., Kohno K., Ohta K., Tutui, Y., Yamada T., Carilli C. 2000 in preparation
- Kennicutt R.C. Jr 1992, *ApJ* 388, 310
- Madau P., Pozzetti L., Dickinson M. 1998, *ApJ* 498, 106
- McMahon R.G., Omont A., Bergeron J., Kreysa E., Haslam C.G.T. 1994, *MN* 267, L9
- Motohara K., Maihara T., Iwamuro F., Oya S., Imanishi M., Terada H., Goto M., Iwai J., et al. 1998, *Proc. SPIE* 3354, 659
- Ohta K., Yamada T., Nakanishi K., Kohno K., Akiyama M., Kawabe R. 1996, *Nature* 382, 426
- Omont A., McMahon R.G., Cox P., Kreysa E., Bergeron J., Pajot F., Storrie-Lombardi L.J. 1996a, *A&A* 315, 1
- Omont A., Petitjean P., Guilloteau S., McMahon R.G., Solomon P.M., Pécontal E. 1996b, *Nature* 382, 428
- Pahre M.A., Djorgovski S.G. 1995, *ApJ* 449, L1
- Pascarelle S.M., Windhorst R.A., Keel W.C., Odewahn S.C. 1996, *Nature* 383, 45

Petitjean P., Pécontal E., Valls-Gabaud D., Charlot S. 1996, Nature 380, 411

Scheffler R.W., Elsässer H. 1988, Physics of the Galaxy and Interstellar Matter (Berlin: Springer Verlag)

Teplitz H.I., Malkan M., McLean I.S. 1998, ApJ 506, 519

Thommes E., Meisenheimer R., Fockenbrock R., Hippelein H., Röser H.-J., Beckwith S. 1998, MN 293, L6

Yun M.S., Carilli C.L., Kawabe R., Tutui Y., Kohno K., Ohta K. 2000, ApJ 528, in press

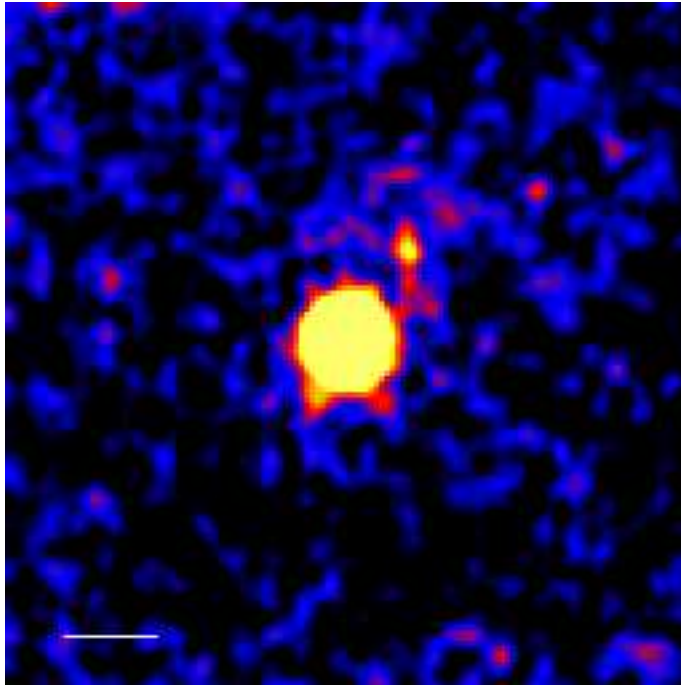


Fig. 1.. Narrow-band image for the redshifted [OII] λ 3727 emission around the quasar BR1202-0725 at $z = 4.7$. Continuum emission is not subtracted. North is at the top and east to the left. A horizontal bar in the left bottom corner shows $2''$ and the displayed field of view is about $15''$. A central brightest object is the quasar. The image is slightly smoothed with a Gaussian kernel for clearer presentation; the FWHM of the quasar in the original image is $0.''55$ and that in the smoothed image is $0.''69$.

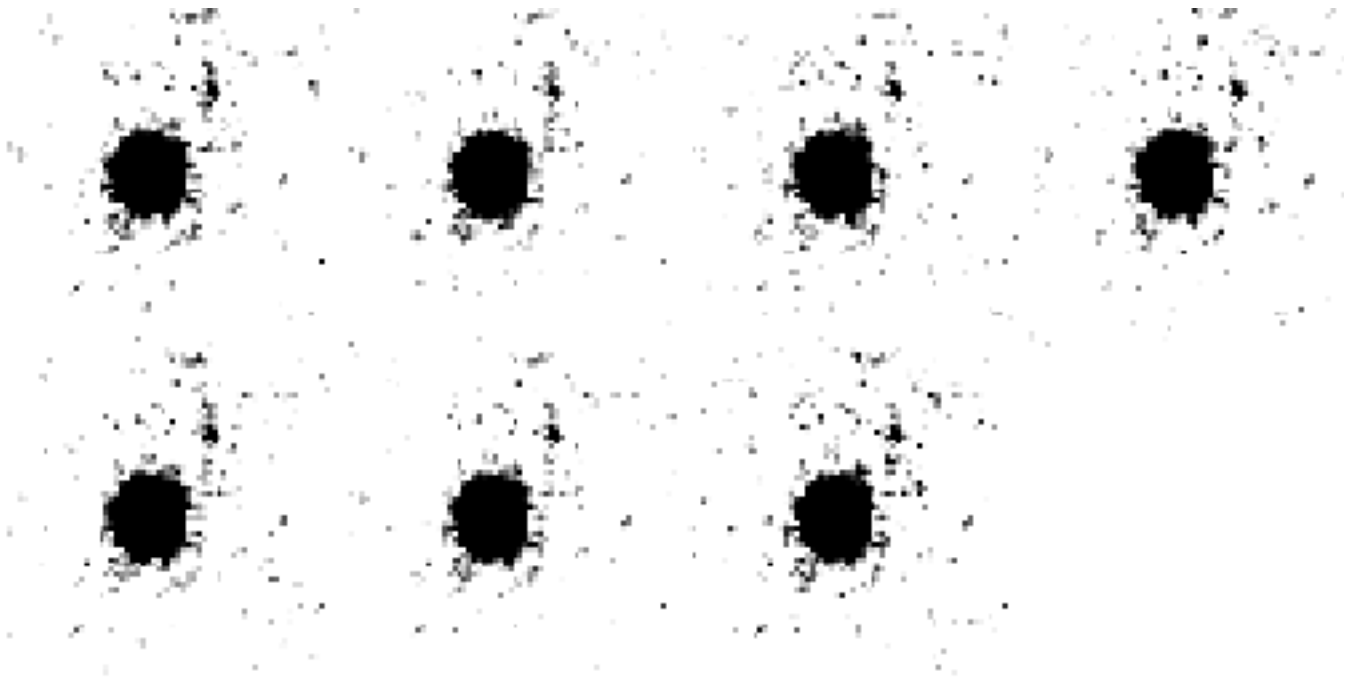


Fig. 2.. Narrow-band images constructed from the frames taken at six telescope pointing. Since we used seven pointing data for figure 1, seven images are obtained. North is at the top and east to the left. No smoothing is applied to these images. All the images show the presence of the companion feature located at $\sim 2.''4$ northwest of the quasar, which indicates the companion feature was not produced by a spurious in a particular position of the detector.

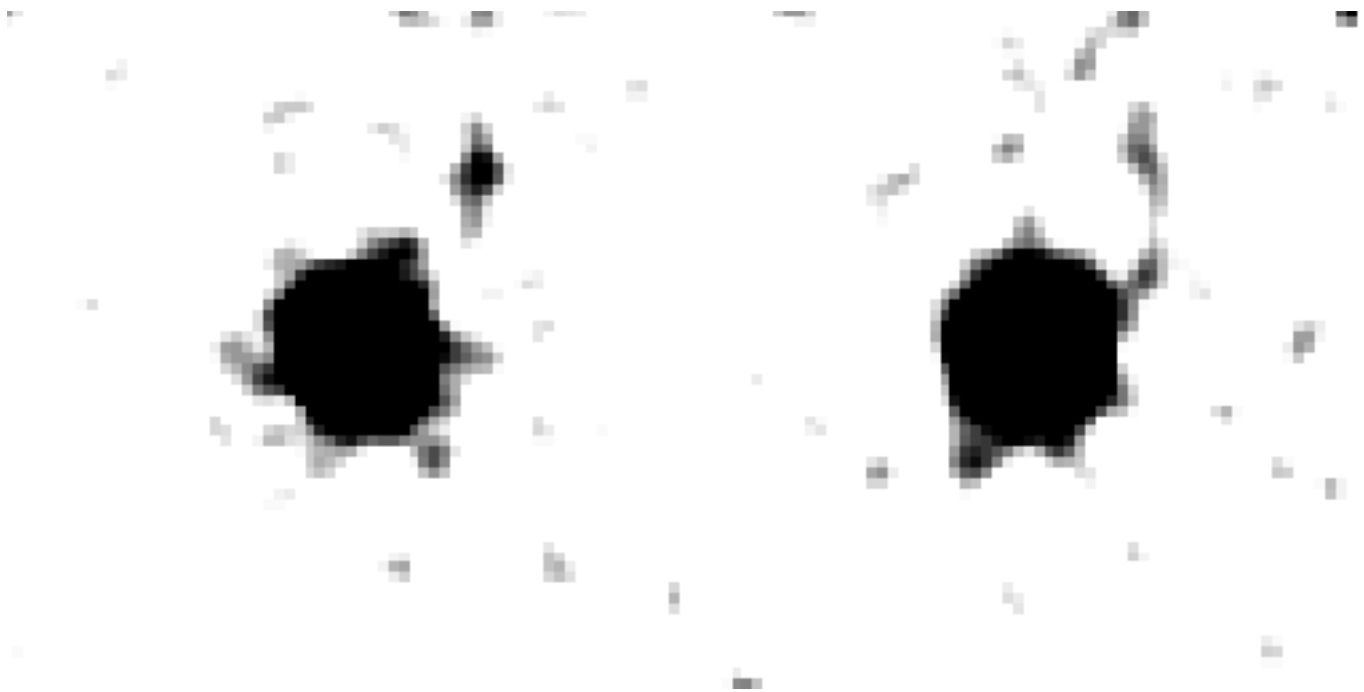


Fig. 3.. The left image is made from frames in which the object locates in the eastern region of the detector, while the right image from frames in which the object locates in the western region of the detector. If the companion feature is a ghost of the quasar, the relative position of the companion to the quasar should depend on the object position in the detector. In both images, the companion feature is located at $\sim 2.''4$ northwest of the quasar, and hence the feature is considered not to be a ghost. Total exposure times of the left and right images are 1050 s and 850 s, respectively.